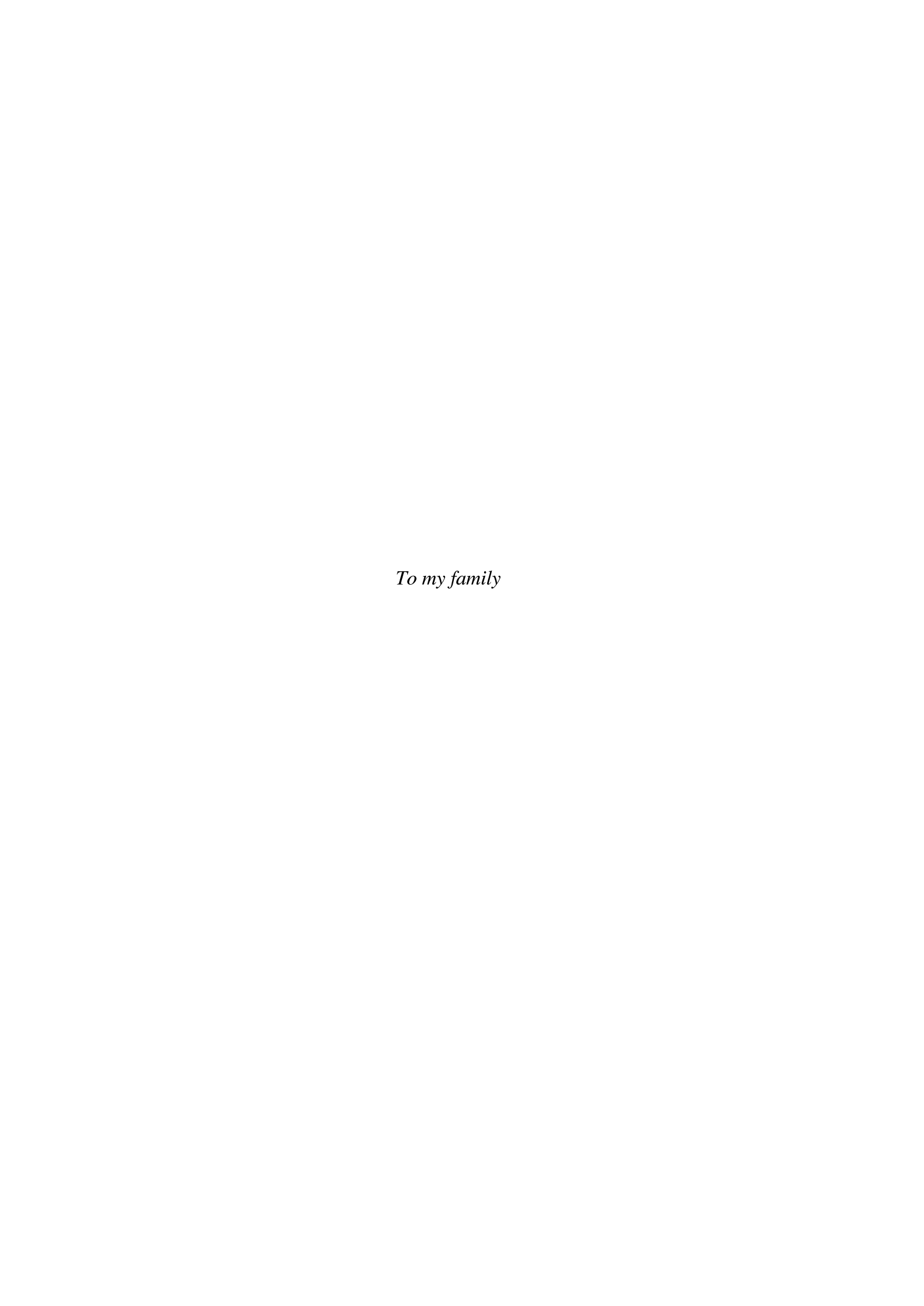
# Experimental studies of the plane turbulent wall jet

by

Jan Eriksson

June 2003
Technical reports from
Royal Institute of Technology
Department of Mechanics
FaxénLaboratoriet
SE-100 44 Stockholm, Sweden

Akademisk avhandling som med tillstånd av Kungliga Tekniska Högskolan i Stockholm framlägges till offentlig granskning för avläggande av teknologie doktorsexamen fredagen den 14 november 2003 kl 13.15 i Kollegiesalen, KTH, Stockholm. © Jan Eriksson 2003



Jan Eriksson 2003, Experimental studies of the plane turbulent wall jet

Royal Institute of Technology Department of Mechanics FaxénLaboratoriet S-100 44 Stockholm, Sweden

#### **Abstract**

Turbulence measurements have been performed in a plane wall jet at a Reynolds number based on inlet velocity,  $Re_0$ , of approximately 10 000. The initial development as well as the fully developed flow was studied. Two- and three-component laser-Doppler velocimetry (LDV) was used. The objective of high quality near-wall measurements necessitated the use of small measuring volumes, as well as the development and application of specific near-wall data treatment.

Detailed turbulence data up to fourth order were obtained, with measurements down to  $y^+ < 2$  for all three velocity components. The inner peaks in the streamwise turbulence intensity , the shear stress, the turbulent kinetic energy (k) and the production of k were resolved. Estimates of the first terms of the near-wall series expansions of  $u^+$ ,  $v^+$ ,  $w^+$ ,  $uv^+$  and  $k^+$  were obtained. Measurements of the mean velocity down to  $y^+ = 1 - 2$  made possible direct wall shear stress measurements.

Turbulence data from the outer layer of the flow were compared to earlier stationary hot-wire results. Large differences were found in the normal and spanwise turbulence intensities, the shear stress and, consequently, in the turbulent kinetic energy. LDV data was used to demonstrate that SHW measurements in the turbulent wall jet will, for fundamental reasons, be in error even for very moderate  $y/y_{1/2}$ .

Development of methodology for simultaneous 3-component measurements was performed, with partial success. The measures necessary to perform high quality measurements were identified, and proven to require no further development work to implement.

The data set generated during the study covers both the initial development and the fully developed region, with measurements from x = 0 to x/b = 200, and fulfils the two-dimensional conservation equations for mass and momentum. It has consequently been used by other workers for validation of computational codes and turbulence models, and development of improved near-wall turbulence models.

Descriptors: Plane turbulent wall jet, turbulence measurements, LDV, near-wall region

#### **Preface**

This thesis deals with the behaviour and characteristics of the plane turbulent wall jet in still surroundings, and the use of laser-Doppler velocimetry (LDV) to determine mean and fluctuating velocities in that flow field. It is based on the following papers:

- **Paper 1.** Eriksson J; Karlsson R; Persson J (1998) An Experimental Study of a Two-Dimensional Plane Turbulent Wall Jet. Exp Fluids 25: 50-60.
- **Paper 2.** Karlsson R; Eriksson J; Persson J (1993) LDV Measurements in a Plane Wall Jet in a Large Enclosure. Laser Techniques and Applications in Fluid Mechanics, Eds. R.J. Adrian et al., Springer Verlag, Berlin-Heidelberg, pp. 311-332.
- **Paper 3.** Eriksson J; Karlsson R; Persson J (1999) Some new results for the turbulent wall jet, with focus on the near-wall region. Presented at the 8<sup>th</sup> International Conference on Laser Anemometry Advanced and Applications. Rome, September 1999. Organized by University of Rome "La Sapienza".
- **Paper 4.** Eriksson J; Karlsson R (2000) Near-Wall Turbulence Structure in the Plane Turbulent Wall Jet in Still Surroundings. Proc. 10<sup>th</sup> Int Symp on Applications of Laser Techniques to Fluid Mechanics, paper 27.6. Inst Superior Technico, Lisbon Portugal.
- **Paper 5.** Eriksson J; Karlsson R (2001) Highly resolved three-component LDV measurements in the plane turbulent wall jet. 2<sup>nd</sup> Int Symp on Turbulence and Shear Flow Phenomena, KTH, Stockholm.
- **Paper 6.** Eriksson J (2002) The 1995 Wall Jet Experiment. Part 2: Simultaneous Three–Component Measurements. Internal report U 02:38, Vattenfall Utveckling AB, Älvkarleby, Sweden.
- **Paper 7.** Eriksson J; Karlsson R; Abrahamsson H; Johansson B; George WK (2002) Evaluation of Hot-Wire Errors in a Plane Turbulent Wall Jet. Submitted to Experimental Thermal and Fluid Science Journal. (Revised and extended version of a paper presented at the ASME Sixth International Thermal Anemometry Symposium, Victoria University, Melbourne, Australia.)
- **Paper 8.** George WK; Abrahamsson H; Eriksson J; Karlsson R; Löfdahl L; Wosnik M (2000) A similarity theory for the turbulent plane wall jet without external stream. J. Fluid Mech., vol. 425, pp. 367 411.
- **Paper 9.** Eriksson J; Karlsson R (1995) An investigation of the spatial resolution requirements for two-point correlation measurements using LDV. Exp Fluids 18: 393-396.

#### Division of work among authors

Papers 1-6 treat different aspects of two experiments on the plane turbulent wall jet. The first experiment was conceived and planned by RK, who also designed the test rig. JE, RK and JP all took part in the execution of that experiment. The data corrections given in paper 2 were developed by RK and JE. The introductory analysis presented in paper 2 was made under supervision of RK, the extended analysis given in paper 1, including some reanalysis, was made by JE with assistance from RK.

The repeat experiment was planned by JE and RK, and performed by JE and JP. JE was responsible for the analysis of that experiment. Generally, papers 1-5 were written by the first author, with assistance from the co-author(s).

Paper 7 is a joint effort where the two groups have contributed with their respective data, from LDV and hot-wire techniques. JE wrote the parts on joint pdf:s and the analysis of the stationary hot-wire results, and undertook the revision of the manuscript together with RK.

Paper 8 is in all aspects primarily a WKG paper. It is based wholly on his ideas, and he also wrote the paper. JE did an extensive processing of the data from papers 1 and 2, partly under supervision of WKG, and helped out with the interpretation of the LDV data.

Paper 9 reports on some two-point correlation measurements performed when testing the methodology for simultaneous three-component measurements proposed by RK. JE took the measurements. JE and RK wrote the paper.

## **CONTENTS**

| ABS <sup>1</sup> | TRACT        |                             | v   |
|------------------|--------------|-----------------------------|-----|
| PREI             | FACE         |                             | vi  |
| DIVIS            | SION OF WO   | ORK AMONG AUTHORS           | vii |
| СНА              | PTER 1       | INTRODUCTION                | 1   |
| СНА              | PTER 2       | OUTLINE OF WORK             | 4   |
| СНА              | PTER 3       | EXPERIMENTAL APPARATUS      | 5   |
| 3.1              | Wall jet tes | st facility                 | 5   |
| 3.2              | Instrument   | tation                      | 7   |
| 3.3              | Optical set  | i-up                        | 9   |
| СНА              | PTER 4       | SUMMARY OF PAPERS           | 10  |
| 4.1              | Paper 1      |                             | 10  |
| 4.2              | Paper 2      |                             | 12  |
| 4.3              | Paper 3      |                             | 14  |
| 4.4              | Papers 4 a   | and 5                       | 15  |
| 4.5              | Paper 6      |                             | 17  |
| 4.6              | Paper 7      |                             | 19  |
| 4.7              | Paper 8      |                             | 20  |
| 4.8              | Paper 9      |                             | 23  |
| СНА              | PTER 5       | NEAR-WALL SERIES EXPANSIONS | 24  |
| СНА              | PTER 6       | CONCLUDING REMARKS          | 25  |
| ACK              | NOWLEDGE     | EMENTS                      | 27  |
| REF              | ERENCES      |                             | 28  |

## **PAPERS**

| PAPER 1.  An experimental study of a two-dimensional plane turbulent wall jet                                      | 33  |
|--|-----|
| PAPER 2.  LDV measurements in a plane wall jet in a large enclosure  | 47  |
| PAPER 3. Some new results for the turbulent wall jet with focus on the near-wall region                            | 71  |
| PAPER 4.  Near-wall turbulence structure in the plane turbulent wall jet in still surroundings                     | 83  |
| PAPER 5. Highly resolved three-component LDV measurements in the plan turbulent wall jet                           | 97  |
| PAPER 6. The 1995 wall jet experiment. Part 2: Simultaneous three-component measurements                           | 103 |
| PAPER 7.  Evaluation of hot-wire errors in a plane turbulent wall jet  | 127 |
| PAPER 8 A similarity theory for the turbulent plane wall jet without external stream                               | 143 |
| PAPER 9.  An investigation of the spatial resolution requirements for two-point correlation measurements using LDV | 189 |

## **CHAPTER 1**

## INTRODUCTION

A wall jet may be formally defined as "a shear flow directed along a wall where, by virtue of the initially supplied momentum, at any station, the streamwise velocity over some region within the shear flow exceeds that in the external stream" (Launder and Rodi, 1981). The best-known everyday example of a wall jet is probably the automobile defroster where it is used for heat and mass transfer modifications. (That is, to keep the windscreen free from mist and/or ice.) There are numerous other engineering applications of the wall jet in essentially different areas. Some examples are the film-cooling of the liner walls of gas-turbine combustion chambers and of the leading stages of the turbine itself, submerged bottom outlets in hydropower dams, the flow from the main circulation pumps of internal type in boiler water nuclear reactors and room ventilation concepts.

The wall jet is usually thought of as a two-layer shear flow, where the inner layer (from the wall to  $y_m$ , the position of maximum velocity) is qualitatively similar to the conventional turbulent boundary layer, while the outer layer (extending from  $y_m$  to the outer edge of the flow) resembles that of a free jet. The flow situation is sketched in figure 1.1. The interaction of the two layers naturally modifies them as compared to the generic flows. Some examples are: The growth rate of the wall jet is considerably lower ( $\sim 30\%$ ) than that of the plane free jet. The displacement of the position of zero shear stress from the position of maximum velocity, where it would occur in a free jet, to about two-thirds  $y_m$ . The shear stress in the wall region drops off much more quickly than in a boundary layer. The turbulence intensities are higher in the inner layer of the wall jet, including the limiting values at the wall. How this basic combination of wall-bounded flow and free shear flow behaves, and how the two layers interact to determine the development of the wall jet, are of interest also from a more fundamental point of view.

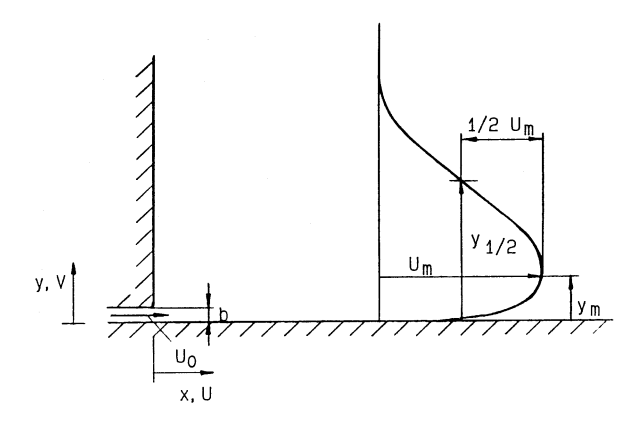


Figure 1.1. Configuration and nomenclature for the plane wall jet.

The wall jet also provides the experimentalist with all the challenges he may wish for. There one finds small scales, large gradients, wall effects, high local turbulence intensity and large

#### 1. INTRODUCTION

anisotropy of the turbulence in the inner layer, and large turbulence intensities (asymptotically - infinite) in the outer layer.

The literature on wall jets is extensive, almost immense. Twenty years ago, at the time of the cornerstone reviews by Launder and Rodi (1981, 1983), well over two hundred experimental studies had been published. More have certainly appeared since then. Considering that, one may well ask the question "Why another wall jet study?" The answer is simply that at the outset of this study, there were still a number of unknowns and unresolved issues in relation to the turbulent wall jet.

Launder and Rodi (1981, 1983) summarized the work on turbulent wall jets up to 1980. They pointed to, among other issues, the measurement of wall shear stress,  $\tau_w$ , as a vexing problem, the lack of definitive data sets on  $\overline{\nu^2}$  and  $\overline{w^2}$ , and that none of the few sets of near-wall  $(y < y_m)$  data for  $\overline{uv}$  was convincing. Figure 1.2, taken from Launder and Rodi (1981), illustrates the amount of spread in the then existing turbulence data. Moreover, turbulence data for the very near-wall region were non-existent.

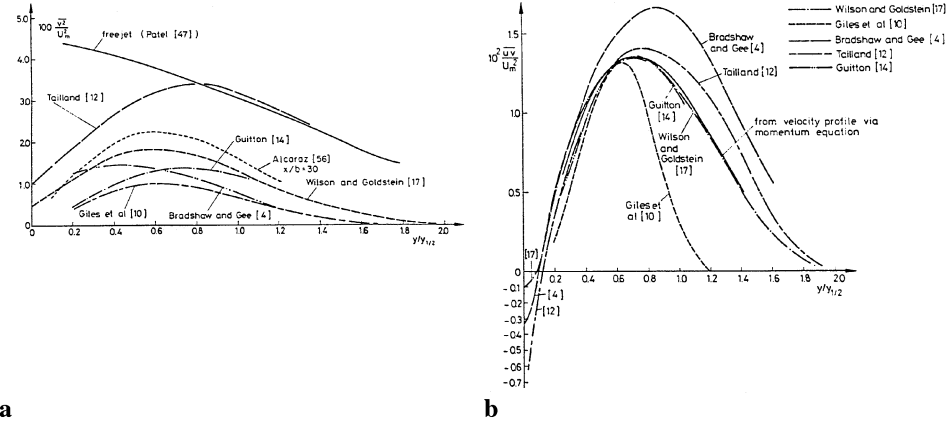


Figure 1.2. Profiles of lateral normal stress (a) and turbulent shear stress (b) across the turbulent wall jet in stagnant surroundings illustrating the amount of spread in the early turbulence data. From Launder & Rodi (1981).

Further work relating to the plane jet in still surroundings was published during the 1980's, Nizou (1981), Nizou et al. (1986)<sup>1</sup>, Schneider (1987) (See also Schneider & Goldstein, 1994), Kobayashi & Fujisawa (1982) and Fujisawa & Kobayashi (1987). Notable here is the work of Schneider, who was the first to use laser-Doppler velocimetry (LDV) for turbulence measurements in the turbulent wall jet. His measurements indicated significantly higher values of  $\overline{w^2}$  over the whole flow and significantly higher values of  $\overline{uv}$  in the outer region, as compared to earlier hot-wire data. He attributed this to problems connected with the use of hot wires in regions with instantaneous flow reversals.

<sup>&</sup>lt;sup>1</sup> Nizou et al. were the first to report on direct wall shear stress measurements in the wall jet using LDV, but their data are likely to be influenced by insufficient spatial resolution and the presence of a return flow.

#### 1. INTRODUCTION

Because of the persisting gaps in the knowledge of the turbulent wall jet, the present work was initiated around 1990. It was explicitly aimed at producing high-quality turbulence data, with special attention to the near-wall region. A secondary objective was to provide a data set suitable for validation of numerical simulations. LDV was the obvious choice for measurement technique due to its superiority when taking turbulence data close to a wall, and its potential to yield accurate results even in very high turbulence intensity flows.

Two major experimental studies were published during the course of the work. Wygnanski et al. (1992) and Abrahamsson (1997) both used hot-wire anemometry (HWA) to study the wall jet in stagnant surroundings. The experiment by Abrahamsson had similar inlet conditions to, and was closely coordinated with, the present work, with an almost continous exchange of results.

#### 2. OUTLINE OF WORK

## **CHAPTER 2**

## **OUTLINE OF WORK**

Essentially all of the papers in this thesis are based on results from two experiments in one and the same test rig. The first set of measurements covered a comparatively long interval in streamwise position but were restricted to two velocity components, meaning that the turbulent kinetic energy could not be determined. The resulting data set was reported in Eriksson et al. (1998) and Karlsson et al. (1993a, 1993b), and are available in the ERCOFTAC Data Base.<sup>2</sup> These data were used as a test case in the ERCOFTAC/IAHR Workshops on Refined Turbulence Modelling in Paris, 1996 and in Delft, 1997.

The repeat experiment was designed and performed to supplement the first data set with three-component measurements at a few streamwise positions in the developed region of the flow. It was also designed to achieve very high spatial resolution for improved near-wall data. Results from the repeat experiment have been reported in Eriksson & Karlsson (2000), Eriksson & Karlsson (2001) and Eriksson et al. (2002).

Results from the two experiments were compared to measurements obtained in the test rig of Abrahamsson (1997) using various hot-wire techniques: stationary, pulsed and flying. Using the LDV technique as a standard, the results were interpreted to understand the limitations of hot-wire techniques in high intensity turbulent shear flows, Eriksson et al. (2002).

The development of experimental methodology and data treatment was a necessary and integral part of the work. This was primarily driven by the objective of high quality near-wall turbulence measurements. The objective of simultaneous 3-component measurements was also a contributory cause. This part of the work is most thoroughly covered in a series of internal reports; Eriksson et al. (1997), Eriksson (2000), Eriksson (2002). Supplementary information is given in Eriksson & Karlsson (2000).

A notable exception to the otherwise purely experimental nature of the thesis is the work reported in George et al. (2000). A similarity theory for the plane turbulent wall jet was formulated, and the data set of Eriksson et al. (1998) and Karlsson et al. (1993a, 1993b) was instrumental in developing and testing that theory.

4

<sup>&</sup>lt;sup>2</sup> ERCOFTAC "Classic Collection" Database, test case C. 55, at http://cfd.me.umist.ac.uk/ercoftac/.

## **CHAPTER 3**

## **EXPERIMENTAL APPARATUS**

The basic flow field that has been studied in this thesis is the two-dimensional wall jet on a plane surface, and more specifically "the plane wall jet in still air" according to the terminology used by Launder and Rodi (1981). There are, however, variations also on this subsection of the wall jet. These variations concern the design of the wall above the inlet. This wall is usually either a thin lip, used e.g. in the experiment by Wygnanski et al. (1992), or an "infinite" vertical wall as in the present experiment. The latter design is simpler to treat computationally, since it, together with a "no inflow" - upper boundary, results in a single, well-defined inflow boundary with known boundary conditions. It was therefore chosen here, in spite of the inevitable return flow that this configuration generates, a return flow which far downstream of the nozzle changes the character of the jet.

An important criterion in the experimental design was that the spatial resolution should be sufficiently high to allow the wall shear stress to be determined directly from mean velocity measurements. This imposes an upper limit on the ratio of measuring control volume diameter to viscous length scale, but a high enough inlet Re-number must also be retained to allow comparisons with earlier studies. Once water was chosen as the working fluid, due to the absence of seeding problems in low-speed water flows, these considerations led to the present combination of slot width and inlet velocity.

#### 3.1 Wall jet test facility

The test facility is shown in figure 3.1. The test section consists of a large tank into which a jet discharges horisontally along the bottom, through a slot. The tank is 7 m long and 1.45 m wide, with a free water surface. One of the side walls is made of glass, as well as the bottom. Using a glass bottom improves the conditions for near-wall measurements, since its smoothness minimizes the diffuse surface reflections (Johnson & Brown, 1990).

Before the repeat experiment, the test section had to be modified to achieve optical access for the measuring of the spanwise velocity component. Originally, the space between the bottom of the test section and the bottom of the tank was water-filled to decrease the load on the test section glass bottom. A large, slighly oval "box", open at its top and bottom, was now fit into this space and sealed against the surrounding water. Thus a dry space was created immediately under the test section, in which a fiberoptic probe with traversing equipment could be placed. The size and position of the box was restricted both by the positions of the load-bearing beams under the water tank and those under the glass bottom. As a consequence, it was not possible to make spanwise velocity measurements on the centerline.

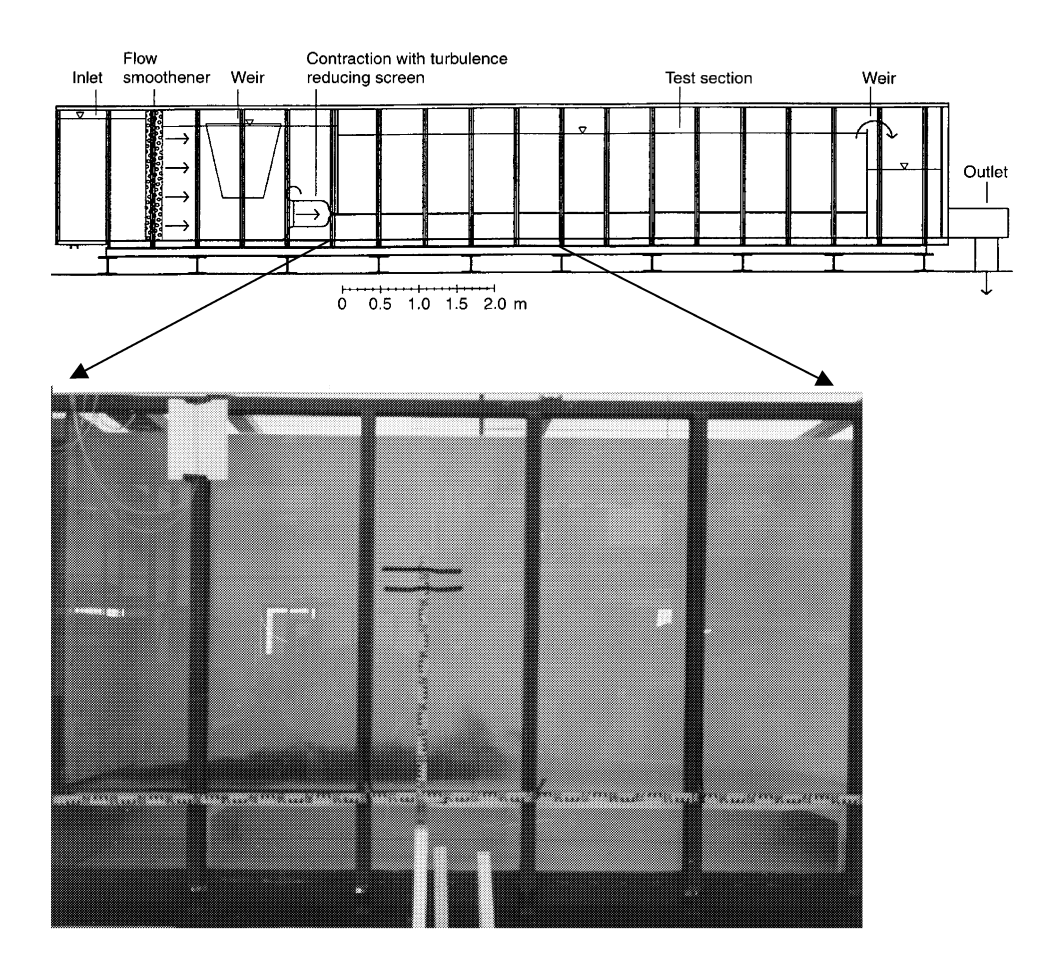


Figure 3.1. Wall jet test facility. a) overview b) test section during preliminary flow visualization

The slot height was initially set as close to 10 mm as possible. It was later re-measured with water in the tank, as part of an effort to close the momentum balance. This was done by a diver, see figure 3.2. The results showed the slot height to be  $9.6 \pm 0.1$  mm over most of the slot width, giving a jet width-to-height-ratio of  $151.^3$  This was considered large enough to obtain good two-dimensionality. A large contraction (Morel 1975, 1977) with a turbulence-reducing screen inserted is used to produce a fairly flat mean velocity profile at the inlet. A weir upstream of the contraction keeps the upstream water level constant, and the flow velocity through the slot is set by an adjustable weir at the downstream end at the tank. This

 $<sup>^3</sup>$  A mean slot height was determined from measurements of the volumetric flow out of the tank vs.  $\Delta h$  (adjusting b to get the correct flow rate), using an experimentally determined inlet velocity profile. The "effective" b was found to be approximately 9.5 mm, which is consistent with the direct determination of the slot height within the experimental uncertainties.

reference velocity is determined as  $U_0 = (2g\Delta h)^{1/2}$ , where  $\Delta h$  is the difference in height between the upstream and downstream free surfaces.

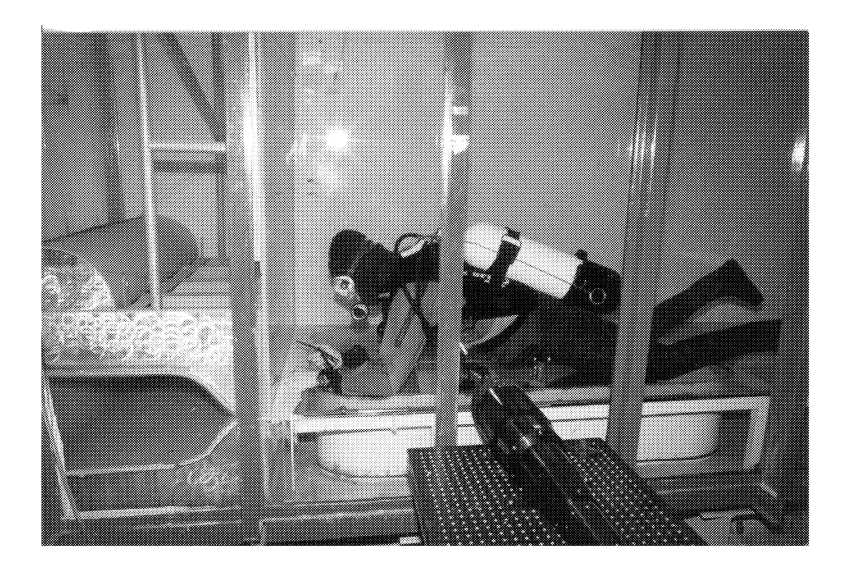


Figure 3.2. Closing the momentum balance. Diver in tank during slot height measurements.

The inlet velocity,  $U_0$ , was set as close as possible to 1 m/s, corresponding to a water depth downstream of the inlet of about 1.4 m. For this water depth, the influence of the recirculating flow on the growth rate of the jet was negligible for the first 150 slot heights.

Using water of approximately room temperature, one obtains a nominal inlet Re-number Re<sub>0</sub> =  $U_0b/v \approx 9.6 \times 10^3$  which is sufficiently high to be comparable to previous experimental studies, e.g. Bradshaw & Gee (1960) and Tailland & Mathieu (1967).

#### 3.2 Instrumentation

TSI LDV hardware was used for all experimental work. Conventional optics was used for the two-component experiment, whereas a fiberoptics system was used in the repeat experiment. In both experiments, an upper-central beam arrangement was used to measure the normal velocity component (V), see Karlsson & Johansson (1988). Standard TSI software was used for data collection and initial data reduction. Silicon carbide particles with a mean diameter of  $1.5 \, \mu m$  was used to uniformly seed the flow.

The first experiment was performed using a modified two-colour system (TSI 9100-7) together with 1980 counter signal processors and frequency shift modules. The system was modified as to increase the beam expansion ratio to 8.5 by including an extra beam expansion module. A front lens with a focal distance of 750 mm was used, in order to reach the centreline of the tank. The probe volume dimensions, based on the  $e^{-2}$  intensity cutoff point, were  $(0.73 \times 0.05)$  mm (streamwise velocity component - 488 nm) and  $(1.60 \times 0.05)$  mm (normal velocity component - 514.5 nm), respectively.

The repeat experiment hardware consisted of a Colorburst for frequency shifting and colour separation, six fiberoptic couplers, two 2-component fiberoptic probes, a Colorlink including receiving optics and frequency mixing electronics, and a 3-component IFA750 signal processor. The fiberoptic probe used to measure the streamwise and normal velocities was equipped with an extra 2.6x beam expander. A front lens with a focal distance of 450 mm was used. (Enough to reach the spanwise positions where 3-component measurements were possible, while still giving small probe volumes.) The resulting probe volume dimensions, based on the  $e^{-2}$  intensity cutoff point, were  $(0.37 \times 0.038)$  mm (streamwise velocity component - 488 nm) and  $(0.78 \times 0.040)$  mm (normal velocity component - 514.5 nm), respectively. The probe used to measure the spanwise component had no extra beam expansion. The front lens focal distance was 250 mm, resulting in a  $(0.74 \times 0.054)$  mm measuring volume (476 nm).

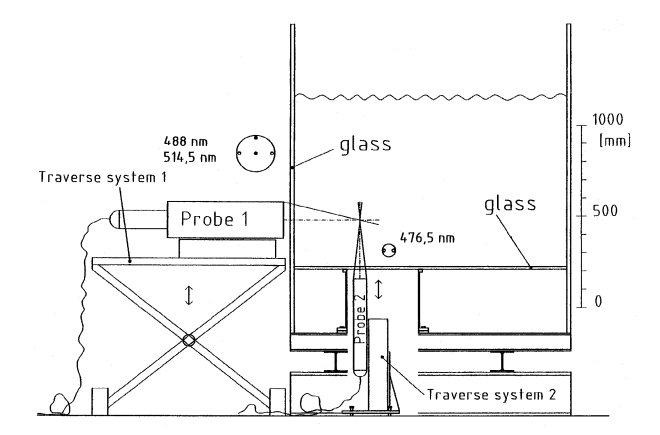
The optical parameters at x/b = 70 are summarized in table 1. The ratio of probe volume diameter to viscous length scale  $(d_{pv}/l^+)$  is included. It is seen that  $d_{pv} \sim 1$  viscous unit at this streamwise position. Since  $l^+$  increases with increasing x/b, the spatial resolution will improve accordingly. (And vice versa for decreasing x/b.)

|                 |                            | Normal velocity | Streamwise velocity | Spanwise velocity |
|-----------------|----------------------------|-----------------|---------------------|-------------------|
| Two-component   | λ (nm)                     | 514.5           | 488                 |                   |
| experiment      | d <sub>pv</sub> (μm)       | 49              | 46                  |                   |
|                 | l <sub>pv</sub> (mm)       | 1.20            | 0.55                |                   |
|                 | Fringe distance (µm)       | 6.18            | 2.89                |                   |
|                 | $d_{pv}/l^+$               | 1.19            | 1.12                |                   |
| Three-component | λ (nm)                     | 514.5           | 488                 | 476               |
| experiment      | $d_{pv}\left(\mu m\right)$ | 40              | 38                  | 54                |
|                 | l <sub>pv</sub> (mm)       | 0.78            | 0.37                | 0.74              |
|                 | Fringe distance (µm)       | 3.76            | 1.80                | 2.48              |
|                 | $d_{pv}/l^+$               | 0.99            | 0.94                | 1.33              |
|                 |                            |                 |                     |                   |

Table 3.1 Optical parameters at x/b = 70.

#### 3.3 Optical set-up

Figure 3.3 shows the experimental set-up for the three-component measurements, but is also useful for illustrating the two-component set-up since the latter is obtained simply by excluding probe 2 and traverse system 2 (and substituting conventional optics for probe 1). A three-axis traverse table was positioned in front of the test section. When running the two-component experiment, the entire LDV system was mounted on this traverse table, Consequently, backscatter light collection was used. For the repeat experiment, the traverse table was used to traverse the fiberoptic probe measuring the streamwise and normal velocities.



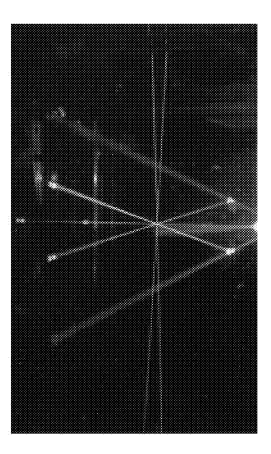


Figure 3.3 Cross-section of wall jet test facility showing experimental set-up for three-component measurements (indicated water depth not to scale).

The probe used to measure the spanwise component was mounted vertically on a one-axis traverse system positioned under the test section. All three-component measurements were made using light collection in 90° side-scatter (scattered light from probe 1 collected through probe 2 and vice versa), meaning that the length of a measuring volume was significantly shorter than the length of the corresponding probe volume;  $l_{mv} << l_{pv}$ . For the optics used,  $l_{mv}$  is reduced to approximately two times the diameter of the orthogonal probe volume. Avoiding direct backscatter light collection also improves the signal-to-noise ratio for all velocity components close to the wall, due to less stray reflections from interfaces between media with different refractive indices.

## CHAPTER 4 SUMMARY OF PAPERS

#### 4.1 Paper 1

Paper 1 is the main experimental paper of the thesis. It gives a complete account of mean velocities and turbulence quantities up to second order moments from the two-component experiment, including initial conditions, growth rate, and decay of streamwise mean velocity. Measurements were taken at x/b=5, 10, 20, 40, 70, 100, 150 and 200, so data from the initial development as well as from the fully developed flow is included. The data are shown to fulfil the two-dimensional momentum equation up to x/b=150, thereby producing strong evidence for the two-dimensionality of the flow as well as for the internal consistency of the measurements. The data are also compatible with the two-dimensional continuity equation, given the difficulties making correct measurements of the normal mean velocity. (The agreement with the continuity equation is shown for one profile, more details are given in paper 8.)

The most important results from paper 1 are the inner layer measurements. To the best of the authors knowledge, these are the first turbulence data ever published for the near-wall region of the turbulent wall jet. It is also, we think, the first correct direct wall shear stress measurements.

A very important feature is the well resolved near-wall layer. It is seen from figure 4.1 that U was measured down to  $y^+ = 1 - 2$ . This resolution is necessary if  $\tau_w$  is to be determined from measurements of the velocity gradient at the wall, since  $U^+$  is linear in  $y^+$  out to  $y^+ = 3 - 4$ , only. The collapse of the profiles gives credibility to the wall shear stress measurements since any non-systematic errors in these measurements would tend to pull the profiles apart.

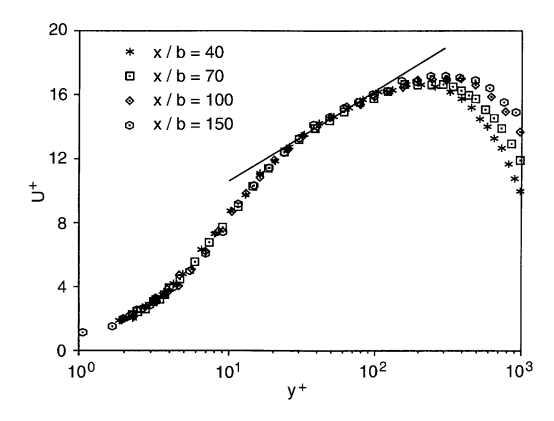


Figure 4.1. Mean velocity profiles in inner scaling,  $U^{\dagger} = f(y^{\dagger})$ .

Figure 4.2 shows local skin friction coefficients versus  $Re_m = U_m y_m/v$ . The correlation proposed by Bradshaw & Gee (1960), and recommended by Launder & Rodi (1981), is shown for comparison, as well as data from Abrahamsson et al. (1994), Wygnanski et al. (1992) and Tailland & Mathieu (1967).

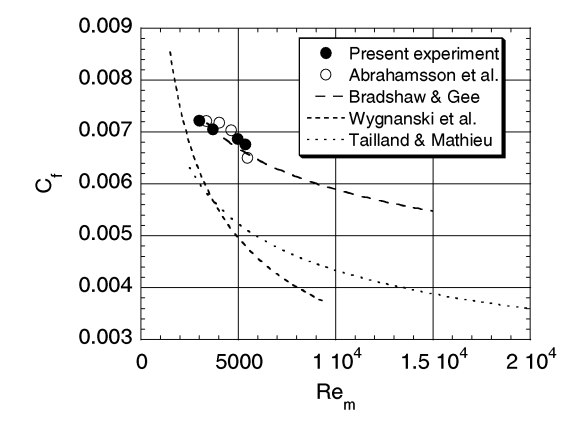


Figure 4.2. Local skin friction coefficients. Comparison to literature data.

The present data is in the range of the Bradshaw & Gee correlation in the limited range of Renumbers studied, but shows a different Re-number dependence. They are also in reasonable agreement with the data of Abrahamsson et al. (Preston tubes). In partial contrast to this, LR81 noted that the then existing determinations of  $C_f$  based on direct measurements of the velocity gradient at the wall produced values ranging from 20% to 35% below the consensus of the impact-tube data. The data from Wygnanski et al. (1992) and Tailland & Mathieu (1967) do show considerably lower skin friction coefficients than the present investigation. In both those investigations,  $C_f$  was determined from hot-wire measurements of the mean velocity near the surface, but using considerably larger values of  $y^+$  for the estimation.  $^4$ 

Concerning turbulence quantities, it can be clearly seen from figure 4.3 that the scaled streamwise turbulence intensity  $u^+$  is dependent on streamwise position (or Reynolds number) outside  $y^+ \approx 8$ , the inner peak level increasing from  $\approx 2.9$  to  $\approx 3.4$ , while the non-dimensionalized shear stress  $uv^+$  collapses out to  $y^+ \approx 100$ . The scaled normal turbulence intensity collapses out to  $y^+ \approx 30$ . Also shown are the (then) best estimates of the leading terms in the near-wall series expansions of  $u^+$  and  $uv^+$ . Best estimates of the leading terms in the near-wall expansions of  $u^+$ ,  $v^+$ ,  $uv^+$ ,  $uv^+$ ,  $uv^+$  and eventsup are tabulated in a separate section of the thesis.

<sup>&</sup>lt;sup>4</sup> The results of Nizou et al. are not shown, since they correlated their data against another Re-number. Using their correlation to compute local skin friction coefficients for the present experiment give values slightly lower than those actually measured.

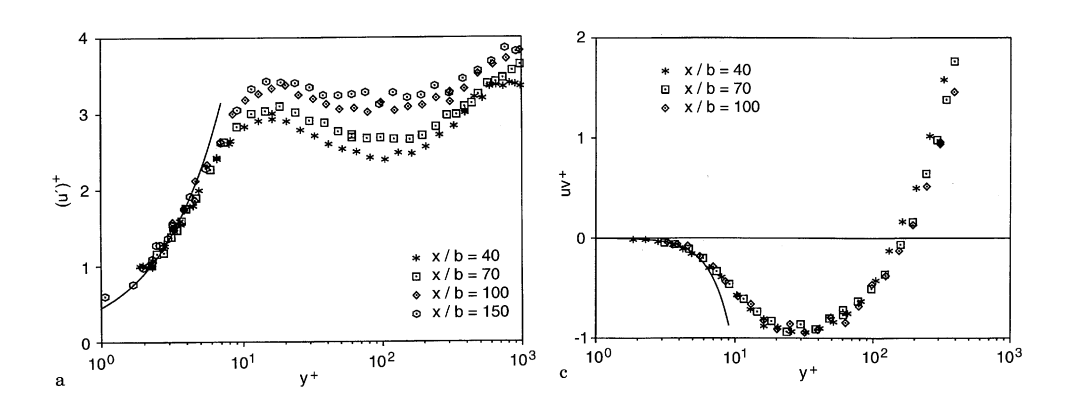


Figure 4.3 Streamwise turbulence intensity and shear stress in inner scaling.

Another important item was the observation of significant differences in the turbulence quantities outside  $y/y_{1/2} \approx 0.5$ , as compared to stationary hot-wire (SHW) data. The peak values in  $\overline{v^2}$  and  $\overline{uv}$  from LDV were higher and positioned further out, with the SHW data going to zero much faster. The high turbulence intensity effects on the hot-wires in the outer flow were proposed as an explanation for these differences. (For clear evidence, see paper 3 and, particularly, paper 7.)

#### 4.2 Paper 2

Paper 2 was a forerunner to paper 1, presenting a small part of the results in preliminary form. It is included in the thesis primarily due to the detailed treatment of data corrections critical to the subsequent work. Essentially all results from paper 2 are included in paper 1. The exception is the skewness and flatness factors of u and v. More definitive results on higher order moments are given in paper 4.

During the first evaluation of the measurements, a number of inconsistencies were observed. The mean normal velocity V was found to be negative over much of the jet profile, which is incompatible with the continuity equation. (A negative  $\partial V/\partial y$  implies an accelerating main flow.) Furthermore, the inner peak in  $uv^+$  was found to be below -1, which is incompatible with the momentum equation.  $(uv^+ < -1)$  is equivalent to  $(uv^+ < -1)$ .

These observations were quite puzzling, and it was not until some time after the experiment that the sensitivity of the measured instantaneous normal velocity to a possible deviation from orthogonality between the beam planes were realized. Correction formulas were derived for V,  $\overline{v^2}$  and  $\overline{uv}$  in terms of an angle error. They were subsequently verified through a repeat of a small part of the measurements with known non-orthogonalities. The LDV system was tilted until reaching a certain angle between the 514 nm-beam plane and the wall normal. Measurements were taken, and the process repeated for a new angle. Figure 4.4 shows the results of this test for V. The actually measured V using a known tilt coincides with the computed contribution to V from U, proving the validity of the correction formula while

<sup>&</sup>lt;sup>5</sup>We are grateful to Prof. Brian Launder for pointing out this fact to us.

simultaneously illustrating the dominating influence of the non-orthogonality on V near the wall. The overlap of the corrected V and the V measured using zero tilt indicates a correctly chosen correction angle. Note finally that an angle error less than  $2^{\circ}$  is enough to make V < 0 all the way out to  $y/y_{1/2}$ .

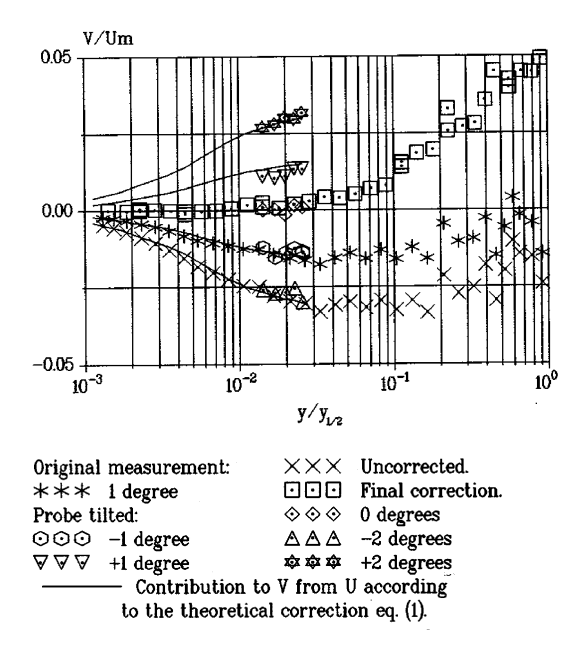


Figure 4.4. Mean normal velocity. Influence of tilt and experimental verification of correction formula.

The correction angle is determined using the conditions  $V^+(0) = 0$ ,  $V^+ \approx a_v y^{+^2}$  close to the wall and  $a_v > 0$ . A corrected  $V^+$  is plotted vs  $y^{+^2}$ . The correction angle is varied until the gradient of a linear fit through the data is as small as possible, but still positive, and the fitted line goes through, or passes as close as possible to, the origin.

Figure 4.5 illustrates the difference between corrected and uncorrected results for an angle error of  $1.7^{\circ}$ . The absolute value of the inner peak in  $\overline{uv}$  is overestimated by more than 20%, whereas the outer peak value is underestimated by 10%. A 0.2° uncertainty in the correction angle will lead to approximately 3% uncertainty in the inner peak value. This clearly shows the importance of an accurate determination of the angle error. An obvious consequence is that measurements as close as possible to y = 0, together with a large number of measurements in the near-wall region, are desirable.

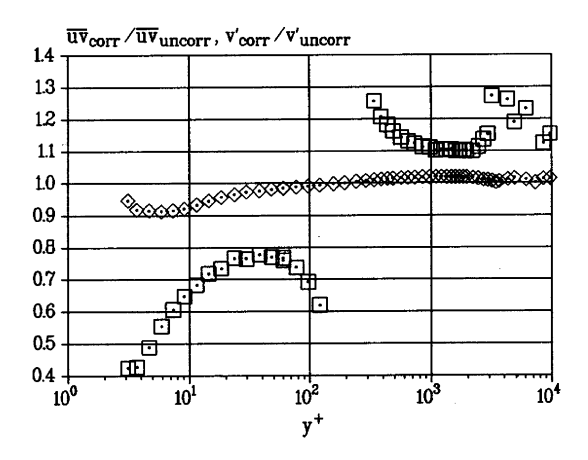


Figure 4.5. Ratios of corrected to uncorrected quantities at x/b = 70. Correction angle =  $1.7^{\circ}$ .

Paper 2 was certainly not the first to treat the issue of non-orthogonality, cf. Morrison et al. (1991). It was, however, especially important here due to the strong anisotropy of the normal stresses near the wall, and an accurate treatment a necessity for the whole investigation.

#### 4.3 Paper 3

Paper 3 presents further results from the two-component experiment. The production term in the k-equation is evaluated. Details on near-wall error sources and connected data corrections are given. The distribution of the direction of the instantaneous flow angle in the x-y-plane is analysed, using angle histograms. It is shown that flow angles outside  $\pm$  45° appears at that y-position where significant differences between SHW and LDV data are first seen. Paper 3 was also the first to combine information from the two- and three-component experiments, presenting a preliminary estimate of the near-wall distribution of turbulent kinetic energy.

The most important subject of paper 3 is the rate of production of turbulent kinetic energy, especially the resolution of the inner peak which was shown for the first time. Figure 4.6 shows the dominant part of the production term,  $-\overline{uv}\left(\partial U/\partial y\right)$ , plotted vs y at x/b = 70. The production rate itself is shown in figure 4.6a, whereas figure 4.6b shows the production rate integrated with respect to y and normalised by the total value of the integral. It is obvious that the inner peak production is much more intense, the ratio of inner peak to outer peak being about 8.<sup>6</sup> The production in the outer shear layer is nevertheless the largest, since it is far less localised. Figure 4.6b shows that more than 85% of the total production takes place in the outer shear layer.

<sup>&</sup>lt;sup>6</sup> Data from the three-component experiment give slightly lower values for the inner peak in  $P^+$ , 0.25 – 0.26 depending on the inclusion or exclusion of individual data points.

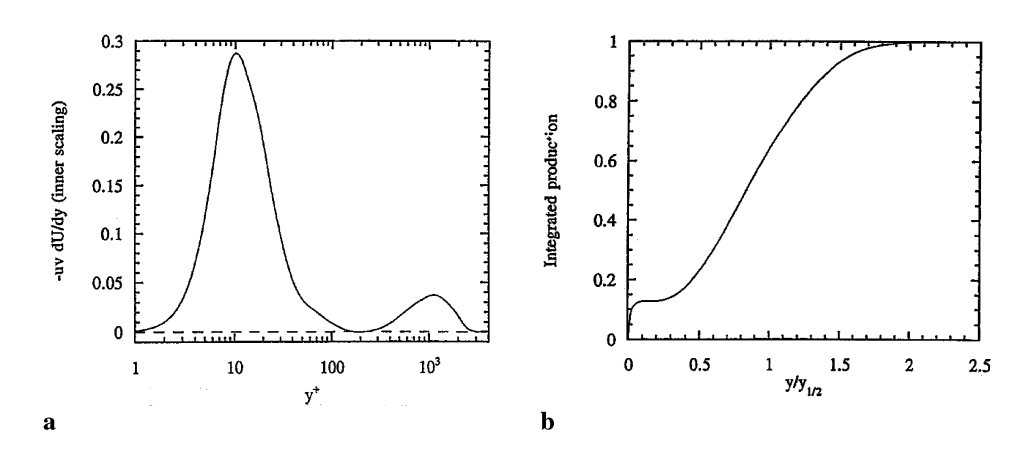


Figure 4.6. Production of turbulent kinetic energy. a) Production rate in inner scaling. b) Integrated production rate.

Including the complementary parts of the production term generally leads only to marginal changes. It does, however, change the sign of the production from negative to positive in a small region near the velocity maximum, so that the total production term stays positive over the whole jet. Irwin (1973) made the same observation for a wall jet in a moving stream with an adverse pressure gradient.

### 4.4 Papers 4 and 5

Papers 4 and 5 present turbulence data up to fourth order moments. Paper 4 focusses on the near-wall region, with detailed measurements down to  $y^+ < 2$  for all three velocity components, compiling all relevant quantities up to fourth order not published earlier. Paper 5 extends the material to the whole wall jet for selected quantities. All data shown in these papers are taken at the streamwise position x/b = 70. Where relevant, comparisons are made to the FPBL data of Karlsson & Johansson (1988) and Johansson & Karlsson (1989).

An important part of paper 4 concerns data treatment relevant to the near-wall region. This comprises discussions of the methodology for simultaneous determination of wall distance and wall shear stress, using a series expansion of  $U^+$  of fourth order in  $y^+$ , and of data refinement related to higher order moments. The methodology used to identify "bad samples" is adopted from Johansson (1988).

Near-wall data on the third and fourth order moments, and an improved turbulent kinetic energy-profile<sup>7</sup>, were the most important results of paper 4. The data on higher order moments had not been available earlier. The k-profile was the first to resolve the near-wall region, and (together with the work of Schneider) the first to provide credible results for the outer region of the jet.

<sup>&</sup>lt;sup>7</sup> This k<sup>+</sup>-profile superseded that published in paper 3. A few new points were added in the very near-wall region, and data refinement completed.

Figure 4.7a shows the turbulent kinetic energy in inner scaling, with the first term in the nearwall expansion of  $k^+$  indicated. The distinguishing features are an inner peak at  $y^+\approx 20$ , a slightly decreasing  $k^+$  over the interval  $20 \le y^+ \le 200$ , and a strong outer peak at  $y^+\approx 1100~(y/y_{1/2}\approx 0.8$  in outer variables). A comparison to figure 4.6a shows that the outer peak coincides with the outer production maximum, while the inner peak is located at twice the wall distance of the inner  $P_{max}$ . Figure 4.7b compares the near-wall k-distribution of the wall jet to that of the FPBL. The profiles are qualitatively quite similar, but the actual levels are about twice as high for the wall jet. Figure 4.8 shows the flatness factors over the whole jet. The general behaviour is much in line with that of the boundary layer, but  $F_u$  and  $F_v$  for the wall jet are considerably higher near the wall.

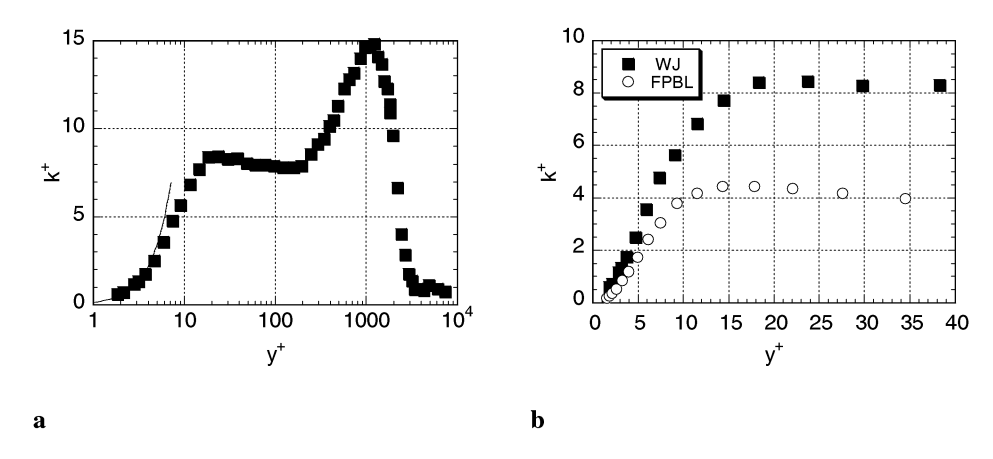


Figure 4.7. Turbulent kinetic energy of the wall jet in inner scaling. a) Entire profile. b) Comparison to FPBL in the near-wall region.

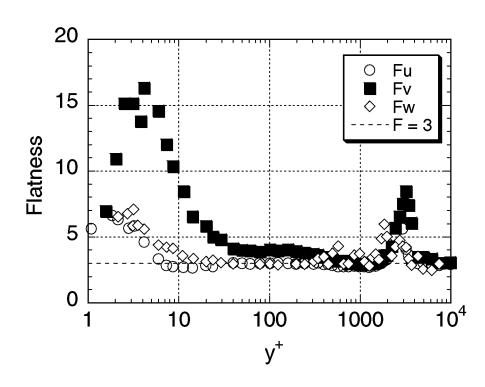


Figure 4.8. Flatness factors for the turbulent wall jet.

#### 4.5 Paper 6

Paper 6 reports on our first serious attempt at *simultaneous* three-component measurements. It is originally an internal report, which is reflected in the style of writing. The paper is detailed, and tries to give a candid account of both achievements and mistakes.

The report treats procedures, results, practical experience and conclusions particular to simultaneous 3-component measurements. Such measurements could be performed as close to the wall as  $y^+ = 4 - 5$ . It was however found to be of great importance to obtain maximum light intensity in the weakest line (476 nm) for the highest possible SNR, both to obtain a high enough data rate and measurements close to the wall. Using a fiberoptic probe fresh from service to transmit the violet light resulted in an order of magnitude increase in data rate for comparable laser power.

A number of confusing differences between results from 2-component - and 3-component measurements were observed. This triggered a detailed analysis of the part of the experimental methodology specific to simultaneous 3-component measurements, particularly with regard to the combination of the system alignment criterion and the signal processor's coincidence criterion. The conclusion was that with the present 3-component set-up, and the present implementation of the coincidence criterion, one will always be in a position where a bias effect tending to sort out low velocity samples may be introduced. This bias effect is basically due to the use of a coincidence window type – coincidence criterion, and subsequently not unique to 3-component measurements. (See e.g. Capp (1983).) The coincidence question is yet more serious for 3-component measurements, since 3 probe volumes have to match. Furthermore, with the 3-component set-up employed, the amount of bias will vary from position to position, due to variations in the flow field *and* the success of the alignment procedure.

Figure 4.9 illustrates the origin of this bias. The indicated particle trajectory will give Doppler bursts ending at different times, the time difference being  $\Delta t$ . The lower the particle velocity, the higher the probability of  $\Delta t$  being larger than the width of the coincidence window. A perfect overlap will eliminate this risk of biasing the measurements, but there is a certain arbitrariness in the positioning of the probe volumes due to the alignment criteria. Besides, in the present experiment different probe volume diameters were used, meaning that there was always a finite  $\Delta x$  (and a finite  $\Delta t$ ). To completely avoid the risk of sorting out low speed particles, a modified coincidence criterion is necessary. This should be seriously considered if 3-component measurements are to be taken in high turbulence intensity flows.

-

<sup>&</sup>lt;sup>8</sup> Fortunately, this appears to be (in principle) very easy to bring about. It has been brought to the attention of the author that the alternative coincidence check outlined in paper 6 for a long time has been "existing technology" (Johansson, personal communication). The so called "master/master hardware coincidence mode" employed in the DANTEC Burst Spectrum Analyzer gives exactly the desired behaviour. Refer to (DANTEC, 1987).

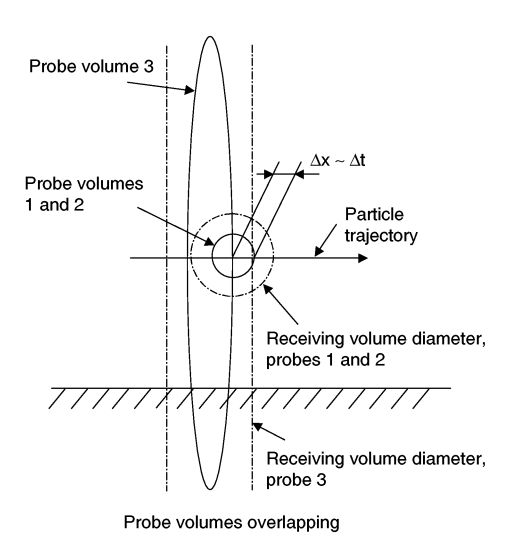


Figure 4.9. Probe volume crossing. All probe volume diameters equal. Receiving volume diameters twice the size of corresponding probe volume diameters. Partial overlap.

Figure 4.10 provides strong evidence for the existence of a coincidence criterion – related bias in the 3-component measurements. Scatter plots of streamwise and normal instantaneous velocities taken from 2- and 3-component measurements at approximately the same wall distance,  $y^+ \approx 4$ , are shown. It is obvious that the very low speed samples are lacking from the 3-component data set.<sup>9</sup>

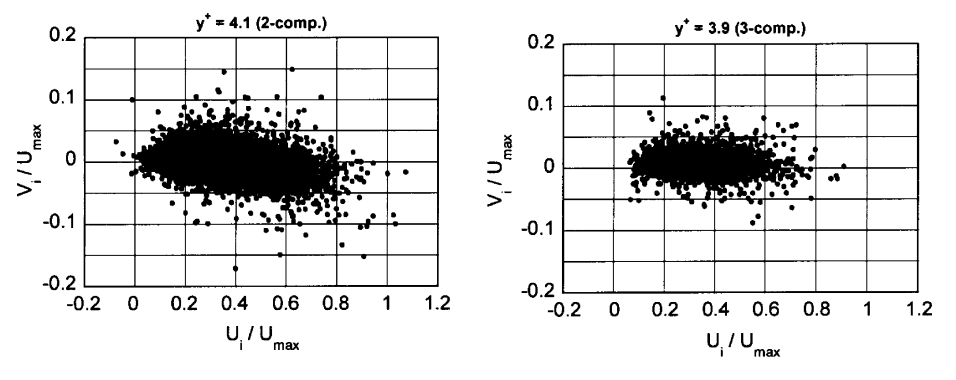


Figure 4.10 Instantaneous velocity pairs.

<sup>&</sup>lt;sup>9</sup> The normal velocities from the 3-component measurements have not been corrected for non-orthogonalities, which is why the "3-component contour" is not tilted.

#### 4.6 Paper 7

This is primarily a paper about the effects of high turbulence intensity on stationary hot-wire measurements in the plane wall jet, although perhaps from an unusual point of view. We do not make any direct quantitative analysis of hot-wire results. Instead, we use LDV data both to demonstrate that SHW measurements will, for fundamental reasons, be in error even for very moderate  $y/y_{1/2}$ , and to indicate the magnitude of the errors in the second order moments. In other words, the LDV data are taken as a standard, these measurements having been shown to be consistent with both the integral and differential equations for momentum and continuity (paper 8).

Figure 4.11 shows the joint probability density function P(u, v) from LDV measurements at the dimensionless wall distances  $y/y_{1/2} \approx 0.48$  and 1.00. Also shown in the plots are the lines  $U_i = \pm V_i$ , defining the "working quadrant" of a cross-wire positioned in the x-y – plane and aligned with the streamwise co-ordinate axis. Combinations of velocities falling outside this quadrant cannot be correctly determined, since the unique relationship between the instantaneous velocity vector and the effective cooling velocities is lost. Such samples are seen already at  $y/y_{1/2} = 0.48$ . At  $y/y_{1/2} = 1.0$  there is a significant amount of them, and even flow reversals, and, naturally, a further increase for larger  $y/y_{1/2}$ .

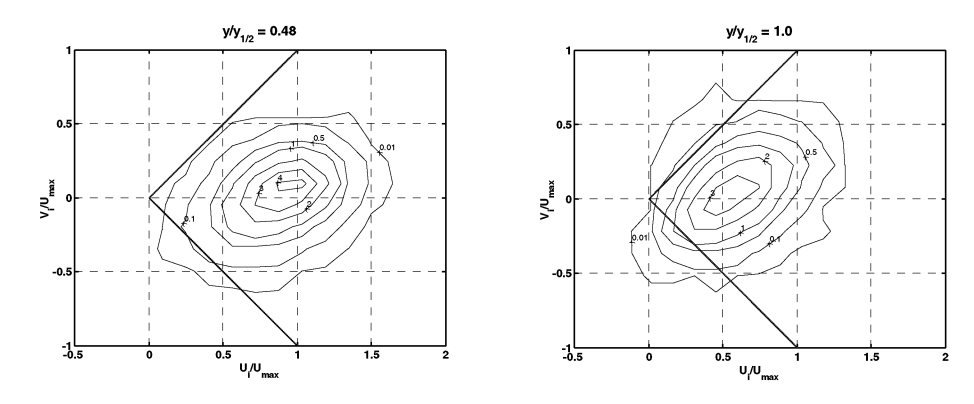
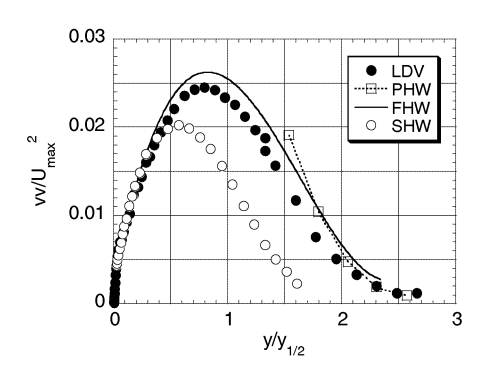


Figure 4.11. Joint probability density functions at  $y/y_{1/2} \approx 0.48$  and 1.00, respectively.

Figure 4.12 compares results from LDV, SHW, FHW and PHW for  $\overline{v^2}$  and  $\overline{uv}$ . The SHW data fall well below the LDV results in the outer region. This is to be expected since a significant part of the large excursions in the instantaneous normal velocities will be incorrectly determined. It is furthermore striking that differences are first seen at that normal position where samples outside the lines  $U_i = \pm V_i$  first occurs. Finally, a comparison to figure 2 reveals that the SHW data of Abrahamsson are "typical" in the sense that they do not stand out from the results of older hot-wire studies.

-

 $<sup>^{10}</sup>$  Assuming a  $\pm$  45° acceptance angle is equivalent to assuming an ideal cross-wire (no prong support interference, symmetrical sensitivity) with a pure Cosine law – response. Real cross-wires lose their directional sensitivity for smaller instantaneous flow angles due to their finite length and end losses to the prompts, see e.g. Shabbir et al. (1987).



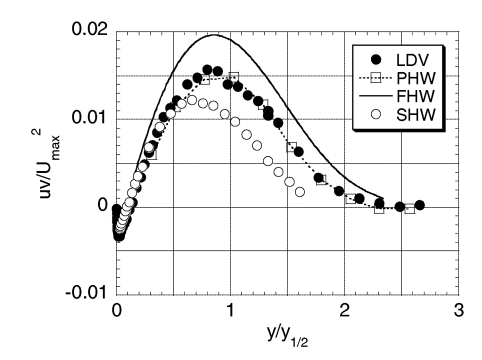


Figure 4.12.  $\overline{v^2}$  and  $\overline{uv}$  in outer scaling. Comparison of results from four different measurement techniques.

An explicit conclusion from this work is that SHW measurements in wall jets should be viewed with considerable caution for  $y/y_{1/2} \ge 0.5$ . An obvious implication is that this paper casts doubt on essentially all older wall jet studies, at least as far as turbulence properties are concerned.

#### 4.7 Paper 8

A similarity theory for the turbulent plane wall jet without external stream is formulated using the asymptotic invariance principle (George, 1995). Appropriate velocity and length scales for the inner and outer equations are determined by requiring that all terms in the infinite Reynolds number equations have the same x-dependence. These scales are used to construct velocity and Reynolds stress profiles that are valid for all y for finite Reynolds numbers, and in the limit of infinite Reynolds number reduce to similarity solutions for the inner and outer equations, respectively. For finite Reynolds numbers, these profiles are shown to retain a dependence on the ratio of the outer and inner length scales (or local Reynolds number), eg.  $U/u^* = f_i(y^+, \delta^+)$  or  $U/U_m = f_o(\bar{y}, y_{1/2}^+)$  where  $\delta^+ \equiv y_{1/2}^+ = u_* y_{1/2} / v$ . This means that they can never collapse perfectly, since  $y_{1/2}^+ = y_{1/2}^+(x)$ .

The fact that both inner and outer scaled profiles,  $f_i$  and  $f_o$ , describe the entire flow for finite Reynolds numbers, but reduce to inner and outer profiles in the limit of infinite Reynolds number, is used to determine both that there is, in the limit, indeed an "overlap" region where both profiles describe the flow *and* to determine their functional forms as a power law behaviour. The theoretical friction law is also a power law, the power and coefficients dependent on the local Reynolds number  $y_{1/2}^+$ . Figure 4.13 illustrates the agreement of the latter with experimental data. (Note that the first two data points relate to the developing part of the wall jet.)

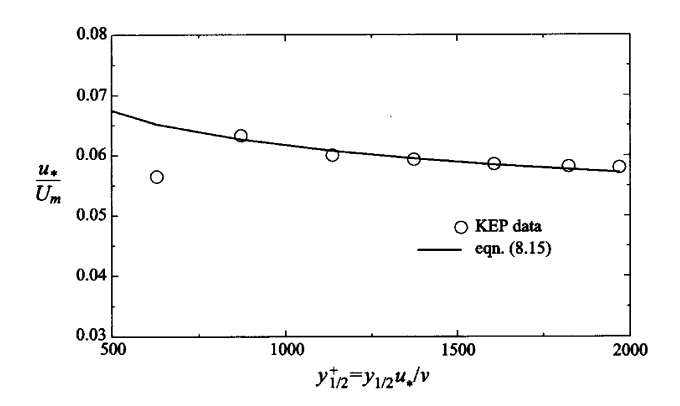


Figure 4.13. Friction velocity vs local Reynolds number. Theoretical friction law and experimental data.

It is inferred from the momentum equation that the velocity maximum and the half-width is related through the condition  $U_m \sim (y_{1/2})^n$ . Available experiments suggest that n may be universal. It is argued using the similarity form of the momentum equation that -n > 1/2. It follows from similarity arguments that as a consequence,  $y_{1/2}$  must grow slower than linearly with x. Based on available experimental data, the asymptotic  $(y_{1/2}^+ \to \infty)$  variation is shown to be nearly linear, but not quite, the exponent being 0.97.

It is also hypothesized that the inner part of the wall jet and the inner part of the zero-pressure-gradient boundary layer are the same. The experimental data appears to support this hypothesis.

Theoretical relations for the X-dependence of  $Y_{1/2} \equiv M_0 y_{1/2}/v^2$  and  $vU_m/M_0$  are derived, where X is defined as  $X \equiv xM_0/v^2$ . (Momentum/viscosity scaling of plane wall jets were first suggested by Narasimha et al., 1973.) Figures 4.14a and 4.14b show the variation of the half-width with downstream distance for the data of Karlsson et al. (1993a, b), Abrahamsson et al. (1994) and Wygnanski et al. (1992), using traditional normalization and momentum/viscosity scaling, respectively. It is clear that the latter scaling works somewhat better. The theoretical curve is included in figure 4.14b. (B<sub>1</sub> is the coefficient in the similarity condition for  $y_{1/2}$  and  $U_m$  in momentum/viscosity scaling.  $C_0$  is the parameter appearing in the explicit form of  $f_0$ .) The agreement between data and theory is excellent.

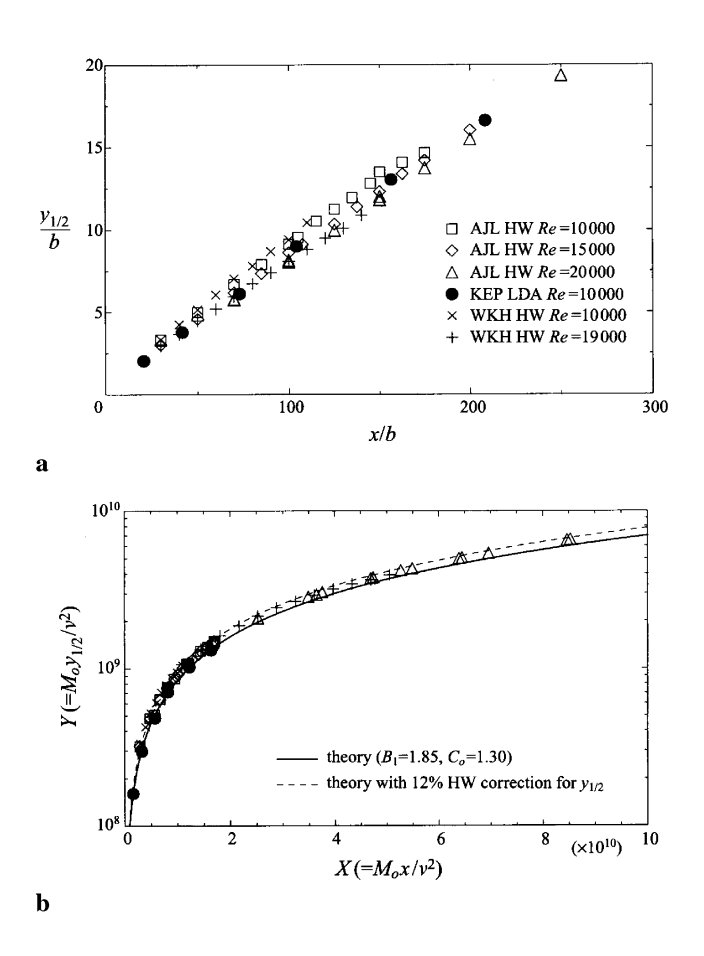


Figure 4.14. Variation of half-width with downstream distance. a) Traditional normalization. b) Momentum/viscosity scaling.

It furthermore follows from the similarity theory that profiles of V/U<sub>m</sub> in the outer region should collapse when normalized with  $(u_*^2/U_m^2)$ . Figure 4.15 shows the actual profiles plotted vs  $y/y_{1/2}$ , together with the profiles computed from the similarity form of the outer-variables version of the continuity equation using data from the x/b = 70-position for the U/U<sub>m</sub> profile. Also shown is the theoretical limiting value for the entrainment velocity. The agreement with the theoretical values is generally satisfying, given the experimental difficulties involved. Similarity breaking down for x/b = 150 is expected, due to the influence of the return flow. The behaviour for x/b = 100 could be due to the loss of similarity already at that position, but from considerations of the momentum equation it appears more likely to be caused by uncertainties in the V measurements.

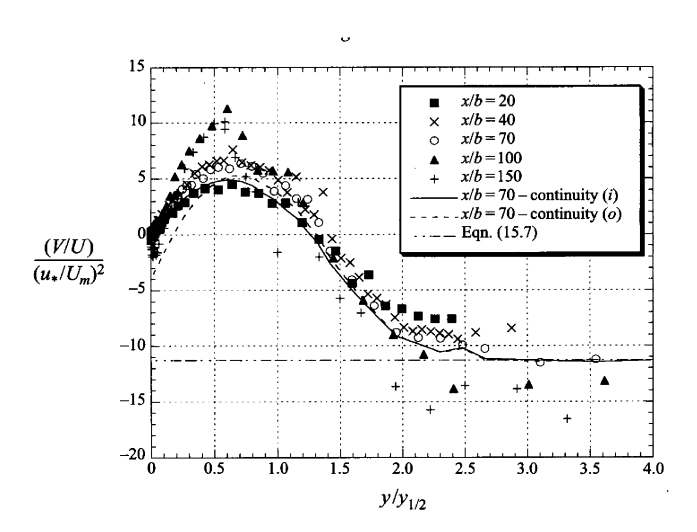


Figure 4.15. Profiles of  $(V/U_m)/(u_*^2/U_m^2)$ .

By way of conclusion, it is stated that determining exactly the asymptotic values of the parameters of the similarity theory, and whether there are features of the initial conditions that are preserved, will require Reynolds numbers well above any experiments to-date.

#### 4.8 Paper 9

This paper reports on spatial correlation measurements performed in connection with the testing of methodology for simultaneous three-component measurements. Measurements with different ratios of characteristic measuring control volume size (d') to Kolmogorov length scale ( $\eta \equiv (v^3/\epsilon)^{1/4}$ ) were used to formulate a simple criterion for the spatial resolution necessary for two-point correlation measurements at small separation. Using the estimate  $\epsilon \sim u^3/l$  to determine  $\eta$ , it was found that  $d'/\eta \leq 1$  could be taken as a practical guideline. The study was limited in scope, and the influence of other parameters, such as coincidence window setting, was not investigated.

Results from measurements of the longitudinal correlation coefficient  $R_{11}(r,0,0)$  on the centerline of a circular jet, starting at x/D=5 where x is the axial distance from the nozzle exit, were presented. Reynolds numbers 85000 and 25000 based on nozzle diameter (D) were used.  $R_{11}$  was clearly negative for a considerable range of r. The longitudinal integral length scales were essentially the same,  $\Lambda_f=0.28$  D, for both Reynolds numbers. This is in line with earlier findings, e.g. Bradshaw et al. (1964) and Sami et al. (1967). The Taylor microscale,  $\lambda_f$ , was found to be one order of magnitude larger than the estimated  $\eta$ .

## **CHAPTER 5**

## **NEAR-WALL SERIES EXPANSIONS**

Slightly different estimates of the first terms of the near-wall Taylor series expansions of  $u^+$ ,  $v^+$ ,  $w^+$ ,  $uv^+$  and  $k^+$  have been reported during the course of the work. The data given in table 2 are the final estimates, arrived at after a renewed analysis of the relevant parts of the very near-wall measurements of both experiments. The second non-zero term, which is also the first non-trivial term, in the  $U^+$ -expansion is included. Its value indicates the degree of internal consistency of the data, since it follows from the near-wall form of the momentum equation that  $c_{uv} = 4d_U$ . <sup>11</sup>

The uncertainty estimates of  $u^+$  and  $w^+$  represents scatter in data points, whereas the indicated intervals for  $uv^+$  and  $U^+$  represents scatter between data series. The uncertainty estimate of  $v^+$  represent scatter due to different assumptions about noise in the data.

|  | Numerical valu    | e of               | Order in y <sup>+</sup> |                                    |
|--|-------------------|--------------------|-------------------------|------------------------------------|
|  | coefficient       |                    |                         |                                    |
| $\mathbf{u}^{+}$   | $0.45 \pm 0.02$   | $(a_u)$            | 1:st                    |                                    |
| $\mathbf{v}^{+}$   | $0.008 \pm 0.002$ | $(b_v)$            | 2:nd                    |                                    |
| u <sup>+</sup> v <sup>+</sup> w <sup>+</sup> uv <sup>+</sup> | $0.265 \pm 0.015$ | (a <sub>w</sub> )  | 1:st                    |                                    |
| $uv^{+}$   | -0.00110.0016     | (c <sub>uv</sub> ) | 3:rd                    |                                    |
| $\mathbf{U}^{+}$   | -0.00030.0004     | (d <sub>U</sub> )  | 4:th                    |                                    |
| U <sup>+</sup>   | 0.136             | $(b_k)$            | 2:nd                    | Computed as $0.5(a_u^2 + a_w^2)$   |
| $\varepsilon_{\mathrm{w}}^{+}$                               | 0.272             |                    | 0:th                    | Computed as $(a_u^2 + a_w^2)^{12}$ |
|  |                   |                    |                         |                                    |

Table 5.1. Leading terms in near-wall series expansions.

<sup>&</sup>lt;sup>11</sup> For more details on near-wall asymptotic behaviour of turbulence statistics, see e.g. So et al. (1991).

<sup>&</sup>lt;sup>12</sup> It follows from the k-equation that, at the wall,  $\varepsilon^+ = \partial^2 k^+ / \partial y^{+^2}$ . Therefore,  $\varepsilon_w^+$  can be computed as  $2b_k \approx 0.272$ .

## **CHAPTER 6**

## **CONCLUDING REMARKS**

The original objectives of the work presented in this thesis were the production of improved turbulence data for the plane wall jet, with particular regard to the near-wall region, and the compilation of a complete, and correct, data set for validation of numerical simulations. It is fair to say that these objectives were met in abundance.

Detailed near-wall turbulence data up to fourth order are now available for the first time, with measurements down to  $y^+ < 2$  for all three velocity components. Notable new features are the resolution of the inner peaks in u<sup>+</sup>, uv<sup>+</sup>, k<sup>+</sup> and P<sup>+</sup>, and the near-wall behaviour of the third and fourth order moments. The first terms of the near-wall series expansions of u<sup>+</sup>, v<sup>+</sup>, w<sup>+</sup>, uv<sup>+</sup> and  $k^{+}$  were determined. Measurements of U down to  $y^{+} = 1 - 2$  made possible the first correct direct wall shear stress measurements.

Concerning the outer layer, a number of earlier stationary hot-wire results have been proven erroneous. For fundamental reasons, SHW turbulence data will be in error even for very moderate  $y/y_{1/2}$ .  $v^2$ ,  $w^2$  and  $\overline{uv}$  are seen to be severely underestimated in the outer layer, resulting in a similar underestimation of both k and the production of k (albeit to different degrees). In consequence, the turbulence data collected and published during the course of this work supersede much of the older wall jet data.<sup>13</sup>

The data set generated is complete in the sense that it covers both the initial development and the fully developed region, with measurements from x = 0 to  $x/b = 200^{14}$ , and correct as far as it has been shown to fulfil the two-dimensional conservation equations for mass and momentum. To the satisfaction of the author, it has indeed been used for validation of computational codes and turbulence models (ERCOFTAC/IAHR 1996, 1997), and development of improved near-wall turbulence models (Gerodimos & So, 1997). The data set has also been instrumental in developing and testing a similarity theory for the plane wall jet (George et al., 2000).

The development of methodology and data treatment for very near-wall measurements was successful. Simultaneous determination of wall shear stress and wall distance provides consistent wall friction measurements, with very high repeatability. The conditions employed to determine the influence of deviations from orthogonality between the beam planes on the normal velocity component give normal mean velocities consistent with the continuity equation, and very repeatable shear stress measurements. The 90° side-scatter light collection employed in the repeat experiment gave significantly less noise near the wall, which made possible measurements of V,  $\overline{v^2}$  and  $\overline{uv}$  closer to the wall. A direct consequence of that is an improved angle error determination. Certain very near-wall data corrections were also developed (Eriksson et al., 1997).

<sup>&</sup>lt;sup>13</sup> In addition, growth rates from SHW studies may, for the same fundamental reasons, be questioned. For large enough y/y<sub>1/2</sub>, even mean velocities will be affected, leading to a consistent overestimation of the rate of spread,  $dy_{1/2}/dx$ .

<sup>14</sup> Admittedly, three-component data has been published for x/b = 70 only.

#### 6. CONCLUDING REMARKS

The development of methodology for simultaneous 3-component measurements was partly successful. The said methodology was indeed validated in the sense that ensemble averaged 2-component and 3-component measurements gave on the whole identical results over a certain range in y, and a number of potential improvements relating to the practicability of the measurements were identified. It is however clear that the introduction of a modified coincidence criterion is compulsory to eliminate the risk of biasing the measurements by sorting out low speed particles. Nevertheless, the measures necessary to perform high quality simultaneous 3-component measurements are identified, and no further development work is needed to implement them.

The work reported in this thesis could be extended in a number of ways. Measurements of the spanwise component and the turbulent kinetic energy at more streamwise positions is perhaps the most obvious point.

Generally, measurements at more than one Reynolds number would be desirable. In particular, measurements at significantly higher Reynolds numbers are needed to further test the proposed similarity theory. Such measurements would require a further improved spatial resolution, e.g. for correct wall shear stress measurements. This would most likely involve specifically designed LDV optics.

Applying the laser-Doppler technique to the three-dimensional wall jet might not be seen as a direct continuation of the present work, but the errors observed in the SHW data for the plane wall jet suggest that it would be a valuable exercise. The local turbulence levels are consistently higher in the three-dimensional wall jet (Abrahamsson, 1997), and consequently SHW data are likely to be even more in error for that flow field.

#### **ACKNOWLEDGEMENTS**

## **ACKNOWLEDGEMENTS**

The writing of this thesis took its time, to the point where anyone doubting that it would ever be brought to an end might well be excused. The greater is the satisfaction in finally having completed it.

A number of persons have contributed to my work in various aspects over the years. Only a few are explicitly mentioned here. They were by no means the only ones to support me (in one capacity or the other), but they are, in retrospect, those who meant most.

My foremost thanks goes to Prof. Rolf Karlsson. I owe him much, both in relation to this particular work and to my professional development in general. Rolf initiated our work on wall jets, and in his simultaneous roles as thesis adviser and then department head at Vattenfall Utveckling gave me continuous support and excellent working conditions. Without his encouragement during the final phases of the work, the thesis would certainly never have been completed.

My heartfelt gratitude also to Prof. William K George. His strong support at a very crucial stage was invaluable. Bill also imparted on me the importance of using the governing equations to check measurement results, gave exhaustive answers to a seemingly neverending stream of questions and, on numerous occasions, helped me with the English language.

Gunnar Johansson has taught me a lot concerning all aspects of the laser-Doppler technique. His willingness to share his wide knowledge is much appreciated. It was very important to me, in particular during my early days as an LDV practitioner.

With my former collegue Johan Persson I share the memories of many late nights struggling to take measurements. And now and then actually succeeding ... It was always a pleasure working with you.

The co-operation with Hans Abrahamsson, who carried out a similar wall jet study at Chalmers University of Technology, was ever stimulating. I think both studies benefitted greatly from exchanging results so freely.

I am grateful to Prof. Fritz Bark for originally accepting me as a PhD student, and for never losing his patience with me. (And if he yet did, he never let me know ...)

The main financing body for this work has been Vattenfall AB. The financial support was provided in turns by "Environment and Development", through a program on Energy-related Fluid Mechanics, and "Electricity Generation". Final reporting was financed through the Vattenfall contribution to the Faxén Laboratory, and by Vattenfall Utveckling AB.

Support from NUTEK through their Fluid Mechanics program is acknowledged.

- **Abrahamsson H** (1997) On turbulent wall jets. PhD thesis, Dept. of Thermo- and Fluid Dynamics, Chalmers University of Technology, Göteborg, Sweden.
- **Abrahamsson H; Johansson B; Löfdahl L** (1994) A Turbulent Plane Two-Dimensional Wall Jet in a Quiescent Surrounding. European Journal of Mechanics B. Fluids, Vol. 13, No. 5, pp. 533-556.
- **Bradshaw P; Ferris DH; Johnson RF** (1964) Turbulence in the noise-producing region of a circular jet. J. Fluid Mech. Vol. 19, pp. 591-624.
- **Bradshaw P; Gee MT** (1960) Turbulent Wall Jets with and without an External Stream. Aeronautical Research Council R&M 3252.
- **Capp S** (1983) Experimental investigation of the turbulent axisymmetric jet. PhD thesis, State University of New York at Buffalo.
- **DANTEC** (1987) Instruction Manual, 57N10 Burst Spectrum Analyzer. DANTEC Documentation Department, Scientific Research Equipment Division.
- **ERCOFTAC/IAHR** (1996) Proceedings of the 5<sup>th</sup> ERCOFTAC/IAHR Workshop on Refined Flow Modelling, EDF/NLH, CHATOU (Paris), April 25-26, 1996. Editors: I. Dauthieu, D. Laurence, S. Richoux.
- **ERCOFTAC/IAHR** (1997) Proceedings of the 6<sup>th</sup> ERCOFTAC/IAHR/COST Workshop on Refined Flow Modelling, Delft University of Technology, Delft, The Netherlands. Editors: K Hanjalic, S. Obi.
- **Eriksson J** (2002) The 1995 Wall Jet Experiment. Part 2: Simultaneous Three Component Measurements. Internal report U 02:38, Vattenfall Utveckling AB, Älvkarleby, Sweden.
- **Eriksson J** (2000) The 1995 Wall Jet Experiment. Part 1: Methodology, Data Treatment and Selected Results. Internal report UI 00:02, Vattenfall Utveckling AB, Älvkarleby, Sweden.
- Eriksson J; Karlsson R; Abrahamsson H; Johansson B; George WK (2002) Evaluation of Hot-Wire Errors in a Plane Turbulent Wall Jet. Submitted to Experimental Thermal and Fluid Science Journal. (Revised and extended version of a paper presented at the ASME Sixth International Thermal Anemometry Symposium, Victoria University, Melbourne, Australia.)
- **Eriksson J; Karlsson R** (2001) Highly resolved three-component LDV measurements in the plane turbulent wall jet. Paper presented at the  $2^{nd}$  Int Symp on Turbulence and Shear Flow Phenomena. KTH, Stockholm.

- **Eriksson J; Karlsson R** (2000) Near-Wall Turbulence Structure in the Plane Turbulent Wall Jet in Still Surroundings. Proc. 10<sup>th</sup> Int Symp on Applications of Laser Techniques to Fluid Mechanics (Paper 27.6). Inst Superior Technico, Lisbon Portugal.
- **Eriksson J; Karlsson R; Persson J** (1999) Some new results for the turbulent wall jet, with focus on the near-wall region. Presented at the 8<sup>th</sup> International Conference on Laser Anemometry Advanced and Applications. Rome, September 1999. Organized by University of Rome "La Sapienza".
- **Eriksson J; Karlsson R; Persson J** (1998) An Experimental Study of a Two-Dimensional Plane Turbulent Wall Jet. Exp Fluids 25: 50-60.
- **Eriksson J; Karlsson R; Persson J** (1997) An Experimental Study of a Two-Dimensional Plane Turbulent Wall Jet. Report US 97:17Ö, Vattenfall Utveckling AB, Älvkarleby, Sweden.
- **Eriksson J; Karlsson R** (1995) An investigation of the spatial resolution requirements for two-point correlation measurements using LDV. Exp Fluids 18: 393-396.
- **Fujisawa N; Kobayashi R** (1987) Turbulence Characteristics of Wall Jets along Strong Convex Surfaces. Int. J. Mech.Sci., vol. 29, pp. 311-320.
- **George WK** (1995) Some new ideas for similarity of turbulent shear flows. Proc. ICHMT Symposium on Turbulence, Heat and Mass Transfer, Lisbon, Portugal (1994) (ed. K. Hanjalic & J. Pereira). Begell House.
- George WK; Abrahamsson H; Eriksson J; Karlsson R; Löfdahl L; Wosnik M (2000) A similarity theory for the turbulent plane wall jet without external stream. J. Fluid Mech., vol. 425, pp. 367 411.
- **Gerodimos G; So RMC** (1997) Near-Wall Modeling of Plane Turbulent Wall Jets. J. Fluids Eng., vol. 119, pp. 304 313.
- **Irwin HPAH** (1973) Measurements in a self-preserving plane wall jet in a positive pressure gradient. J. Fluid Mech, vol. 61, part 1, pp. 33-63.
- **Johansson G** (1988) An experimental study of a flat plate turbulent boundary layer, using laser-Doppler Velocimetry. Ph D Thesis, Chalmers University of Technology, Göteborg, Sweden.
- **Johansson TG; Karlsson RI** (1989) The Energy Budget in the Near-Wall Region of a Turbulent Boundary Layer. Applications of Laser Anemometry to Fluid Mechanics, Eds. R.J. Adrian et al. Springer-Verlag Berlin Heidelberg, pp. 3-22.
- **Johnson DA; Brown JD** (1990) A Laser Doppler Velocimeter Approach for Near-Wall Three-Dimensional Turbulence Measurements, Paper 3.2 in Fifth International Symposium on Applications of Laser Techniques to Fluid Mechanics, Lisbon, Portugal.

- **Karlsson R; Eriksson J; Persson J** (1993a) LDV Measurements in a Plane Wall Jet in a Large Enclosure. Laser Techniques and Applications in Fluid Mechanics, Eds. R.J. Adrian et al., Springer Verlag, Berlin-Heidelberg, pp. 311-332.
- **Karlsson R; Eriksson J; Persson J** (1993b) An Experimental Study of a Two-Dimensional Plane Turbulent Wall Jet. Report VU-S 93:B36, Vattenfall Utveckling AB, Älvkarleby, Sweden.
- **Karlsson R; Johansson TG** (1988) LDV Measurements of Higher Order Moments of Velocity Fluctuations in a Turbulent Boundary Layer. Laser Anemometry in Fluid Mechanics III, Eds. R.J. Adrian et al. Ladoan Instituto Superior Tecnico, Lisbon.
- **Kobayashi R; Fujisawa N** (1982) Turbulence Characteristics of Plane Wall Jets. Report No. 352 of the Inst. of High Speed Mechanics, Tohoku University, Sendai, Japan.
- **Launder BE; Rodi W** (1981) The turbulent wall jet. Prog. Aerospace Sci., Vol. 19, pp. 81 128.
- **Launder BE; Rodi W** (1983) The turbulent wall jet measurements and modelling. Ann. Rev. Fluid Mech. pp. 429 459.
- **Morel T** (1975) Comprehensive design of axisymmetric wind tunnel contractions. J. Fluids Eng., vol. 977, pp. 225 233.
- **Morel T** (1977) Design of Two-Dimensional Wind Tunnel Contractions. J. Fluids Eng., pp. 371-378.
- Morrison GL; Johnson MC; Swan DH; De Otte Jr RE (1991) Advantages of orthogonal and non-orthogonal three-dimensional anemometer systems. Flow Measurement and Instrumentation, Vol. 2, pp. 89-97.
- Narasimha R; Yegna Narayan K; Parthasarathy S (1973) Parametric analysis of turbulent wall jets in still air. Aero. J. pp. 355-359.
- **Nizou PY** (1981) Heat and Momentum Transfer in a Plane Turbulent Wall Jet. J. Heat Transfer, vol. 103, pp. 138-140.
- **Nizou PY; Roiland M; Tida Ts** (1986) Velocity Profile and Skin Friction Formulation for a Plane Turbulent Wall Jet. Paper 12.6, Third Int. Symp. on Applications of Laser Anemometry to Fluid Mechanics, Lisbon.
- **Sami S; Carmody T; Rouse H** (1967) Jet diffusion in the region of flow establishment. J. Fluid Mech. vol. 27, pp. 231-252.
- **Schneider ME** (1987) Laser-Doppler measurements of turbulence in a two-dimensional wall jet on a flat plate in stagnant surroundings. Ph.D. Thesis, University of Minnesota.

- Schneider ME; Goldstein RJ (1994) Laser Doppler measurement of turbulence parameters in a two-dimensional plane wall jet. Phys. Fluids, Vol. 6, pp. 3116-3129.
- **Shabbir A; Beuther PD; George WK** (1987) X-Wire Response in Turbulent Flows of High Intensity Turbulence and Low Mean Velocities. Paper presented at the ASME Symposium on Thermal Anemometry, Cincinnati, Ohio, June 1987.
- **So RMC; Lai YG; Zhang HS; Hwang BC** (1991) Second-order near-wall turbulence closures: A review. AIAA Journal 29: 1819-1835.
- **Tailland A; Mathieu J** (1967) Jet pariétal. Journal de Méchanique, Vol. 6, No.1, pp. 103-131.
- Wygnanski I; Katz Y; Horev E (1992) On the Applicability of Various Scaling Laws to the Turbulent Wall Jet. J. Fluid Mech. (1992), Vol. 234, pp. 669-690.